Journal of Superconductivity and Novel Magnetism
https://doi.org/10.1007/s10948-021-05915-w

ORIGINAL PAPER

Effect of Orthorhombicity on the Electronic Structure and Superconducting Properties of High-T_c Cuprate Family

Ilya Anatolyevich Makarov[1] · **Sergey Gennadyevich Ovchinnikov**[1]

Received: 22 April 2021 / Accepted: 8 May 2021

Abstract
Electronic structure in the normal state and properties in the superconducting state of the orthorhombic phase in HTSC cuprates are studied within the multielectron generalized tight-binding (GTB) approach. The joint effect of variation of average Cu-O distance and orthorhombic distortion on the Fermi contour, band structure, and concentration dependence of T_c is studied. Quasiparticle excitations were constructed within the framework of the five-band p-d model for the layer of the CuO_6 octahedra. The electronic structure of quasiparticle excitations in the effective Hubbard model is calculated using the equation of motion for Green's functions in the generalized mean-field approximation. Orthorhombic distortion leads to asymmetric with respect to the nodal direction of the Brillouin zone dispersion surface of quasiparticle excitations and to splitting of each van Hove singularity into two peaks. Transformation of the Fermi contour from hole pockets to the large hole and electron pockets occurs as a result of two quantum-phase transitions at dopings x_{c1} and x_{c2}. Simultaneous average Cu-O distance elongation and orthorhombic distortion decreasing result in T_c decrease. T_c dependence on average Cu-O distance in the orthorhombic phase is in agreement with the behavior of experimental $T_{c\max}$ values when the DOS effect on T_c prevails over the effect of the exchange parameter. There are two T_c maxima in the orthorhombic system with the suppressed exchange parameter, and these maxima appear at concentrations x_{c1} and x_{c2}.

Keywords Cuprate superconductors · Orthorhombic distortion · Strong electronic correlations · Hubbard model · Electronic structure · Concentration dependence of T_c

1 Introduction

As is known, the important control parameter in HTSC cuprates is the concentration of doped carriers in CuO_2 layers. The T_c difference in various representatives of cuprates indicates that there are other factors influencing T_c in addition to doping. The most obvious parameter associated with the main structural element of cuprates, the CuO_2 layer, is the value of the CuO_2 lattice parameter. A strong influence of pressure on T_c also hints at the importance of this parameter since the distance between atoms changes significantly under pressure. Unfortunately, the results of pressure experiments are rather difficult to interpret, and the mechanism of its influence on T_c is ambiguous since pressure P changes several parameters and structural features.

A convenient object for studying the $T_c(P)$ dependence is the mercury family of cuprates due to their simple crystal structure and their stability in a wide range of charge carrier concentrations. The effect of pressure on T_c was studied in cuprates with tetragonal structure $HgBa_2Ca_{n-1}Cu_nO_{2n+2+x}$ in the region of weak, optimal, and strong doping x in [1–13]. A significant effect of pressure is a change in the number of charge carriers in the CuO_2 layers that is the $T_c(P)$ dependence will have a different character at different doping levels. Therefore, it is usually necessary to distinguish between the intrinsic pressure effect associated with a change in the crystal and electronic structure and the effect associated with a change of doped charge carriers quantity [14]. Growth of the number of carriers in the CuO_2 layers occurs when the distance between them and the buffer layer decreases, i.e., when the uniaxial pressure is applied along the c axis. The derivative of T_c with respect to the uniaxial pressure along the c axis changes non-monotonically, reflecting the behavior

✉ Ilya Anatolyevich Makarov
maki@iph.krasn.ru

Sergey Gennadyevich Ovchinnikov
sgo@iph.krasn.ru

[1] Kirensky Institute of Physics SB RAS, Krasnoyarsk 660036, Russia

Published online: 18 May 2021

of T_c with doping: in underdoped compounds $dT_c/dP_c > 0$ since the pressure along the c axis increases the effective number of doped holes, in the region of strong doping an additional growth of the number of the carriers decreases T_c and $dT_c/dP_c < 0$. dT_c/dP_c reacts weakly to a change of hole concentration in the region of optimal doping [15, 16]. At the same time, the derivatives dT_c/dP_a and dT_c/dP_b are almost independent of doping and have a significant value at optimal doping [15]. Therefore, it is believed that the intrinsic mechanism of T_c variation is characterized by the effect of uniaxial pressure in the (a, b) plane in the region of optimal doping.

The study of the T_c dependence on uniaxial pressure along the a and c axes at optimal doping in single-layer mercury cuprate $HgBa_2CuO_{4+\delta}$ (Hg1201) showed that $dT_c/dP_a > 0$ and $dT_c/dP_c < 0$ [17]. $T_{c\,\max}$ increase with optimal doping results from a decrease of the Cu-O distance in the CuO_2 plane and an increase in the distance between the copper atom and the apical oxygen. The conclusions that the area of CuO_2 planes reducing and the distance between them increasing are favorable for superconductivity were confirmed in experiments on uniaxial pressure in $La_{2-x}Sr_xCuO_4$ (LSCO) [18], $Bi_2Sr_2Ca_2Cu_2O_{8+y}$ (Bi2212) [19] and for hydrostatic pressure in [17] and other experiments on mercury cuprates with $n = 1, 2, 3$ [3, 7, 11]. The effect of hydrostatic pressure is weaker [20] than uniaxial since the derivatives of T_c with respect to pressure along the a and c axes have different signs and their influence is partially compensated.

T_c of each representative of the mercury family grows to saturation at a certain pressure which is different for each specific compound [2, 12, 13]. It was shown [13] that there is a correlation between the growth of $T_{c\,\max}$ when the number of CuO_2 layers n increases up to 3, and the decrease in the CuO_2 lattice parameter. Possibly the obtained correlation shows a direct influence of the Cu-O bond length on T_c. At $n > 3$ $T_{c\,\max}$ decreases although the lattice parameter of CuO_2 continues to decrease [13]. Apparently, the latter feature is associated with a change of the carriers number in the CuO_2 layers since an increase the number of CuO_2 layers leads to an inhomogeneous distribution of charges among the outer and inner layers. Since pressure results in a redistribution of charges the effect of pressure on T_c through doping will be significant in multilayer cuprates with $n \geq 3$.

The results of experiments on chemical pressure using anion substitution of oxygen with fluorine atoms in $HgBa_2Ca_2Cu_3O_{8+\delta}$ (Hg1223) agree with the results of experiments on uniaxial pressure regarding the relationship between the Cu-O distance in the CuO_2 plane and T_c [12]. The smaller ionic radius of fluorine leads to compression of the bond between planar copper atom and apical oxygen and decreases the planar Cu-O distance in Hg1223 [1, 7]. Chemical pressure results in an increase in T_c in Hg1223 [12]. Fluorination of Hg1201 also leads to a decrease in the distance between planar copper and apical oxygen but almost does not change the planar Cu-O distance. The fact that T_c in Hg1201 is almost independent of fluorination suggests that the increase of T_c is due to the compression of the CuO_2 planes and the distance to the apical oxygen has a small effect on T_c. A similar change of dT_c/dP_a was obtained using epitaxial deformation of the $La_{1.9}Sr_{0.1}CuO_4$ compound [21].

The cation substitution of Hg atoms in mercury cuprates by Tl atoms with a smaller ionic radius also increases T_c due to CuO_2 plane compression and increased oxygen content in the buffer layers [22–24]. However, the substitution of atoms in the buffer layers does not always have a positive effect on T_c since it affects a large number of mechanisms of influence on T_c. From one side, the in-plane Cu-O bond stretching makes the CuO_2 layer flatter which favors superconductivity. From another side, the replacement of cations with atoms having a large ionic radius stretches the Cu-O bonds in the CuO_2 plane and thus decreases T_c. Since the substitution occurs in random places of buffer layers, out-of-plane disorder [25–28] appears in them. Out-of-plane disorder brings to local lattice distortions and random Coulomb potential which also can reduce T_c.

The behavior of T_c with pressure along the a and b axes is qualitatively different in various representatives of orthorhombic cuprates. dT_c/dP_a and dT_c/dP_b derivatives in $YBa_2Cu_3O_{7-\delta}$ (YBCO) have different values and opposite signs [15, 29]. dT_c/dP_a and dT_c/dP_b in Bi2212 have the same signs but the absolute values can either coincide [30] or to be different [19]. The difference in the values of the derivatives dT_c/dP_a and dT_c/dP_b suggests the presence of dependence of T_c on the orthorhombic distortion $(b - a)$. Experimental manifestations of the nonzero derivative $dT_c/d(b - a)$ were obtained in YBCO in works [16, 31]. In these works, decrease in the orthorhombic distortion $(b - a)$ leads to T_c increasing. The same result of T_c decreasing due to orthorhombic distortion was obtained in the LSCO study [32, 33].

Correlation between T_c and CuO_2 lattice parameters is obvious on the basis of the above experimental data and many other works. This correlation is expressed in two tendencies: T_c decreases with planar Cu-O distance increasing and T_c grows with orthorhombic distortion decreasing. These two tendencies are combined in the dependence of the T_c maxima on the value of the planar Cu-O distance in various cuprates [34] which has the form of a nonmonotonic dome-like curve with a maximum for the Hg1223 compound. It was also noted in [34] that there are characteristic values of the Cu-O distance that separate the regions of the system located in the high temperature tetragonal (HTT) and the low-temperature orthorhombic (LTO) phases. The threshold value of the Cu-O distance separating HTT and LTO also

divides regions with different dependences of the maximum T_c. The maximum of T_c in the HTT phase decreases with the CuO_2 lattice parameter increasing. In the orthorhombic phase, the dependence of T_c on the average Cu-O distance is different: the maximum T_c increases with distance increasing. In the orthorhombic phase, variation of average Cu-O distance is accompanied by a variation of the orthorhombicity factor which is defined by the ratio between lattice parameters a and b. Compounds having higher T_c as the distance grows are characterized by less orthorhombic distortions. The unsolved questions are whether the observed behavior of experimental T_c maxima in different cuprates as a function of various average Cu-O distances can be explained only by the influence of the CuO_2 lattice parameters and their ratio on T_c and what is the mechanism of this influence.

The influence of the CuO_2 lattice parameter on T_c in the HTT phase of cuprates was described in theoretical studies [35, 36] within the t-J model based on the theory of superconducting pairing caused by antiferromagnetic exchange interaction. Effect of the hydrostatic and uniaxial pressure along the c-axis and in the (a, b) plane on the superexchange interaction J was obtained in work [36]. J renormalization under deformations along the c-axis and in the (a, b) plane has different signs, it brings to T_c decreasing in the first case and T_c increasing in the second case according to experimental data. In work [35] estimation of the T_c change with variation of the lattice parameter a was made and the obtained value dT_c/dP_a is close to the experimental data [13]. It was also concluded that the $T_c(a)$ dependence is strong due to the renormalization of the hybridization parameter t_{pd} which determines the magnitude of the indirect exchange interaction.

Besides pairing interaction, there is one more mechanism of influence of Cu-O distance on the T_c, it is the density of states (DOS) mechanism: Crystal structure transformation under pressure induces transformation of electronic structure and DOS that changes T_c. Therefore, it is necessary to solve certain sub-tasks to find out whether the observed behavior of T_c [34] resulted from a change of the Cu-O distance for both the HTT and LTO phases within the unified theory of superconductivity and what role is played by the transformation of the electronic structure which manifests itself in the DOS. These sub-tasks are the study of the properties of the tetragonal phase in (i) normal and (ii) superconducting states and the study of the orthorhombic phase properties in (iii) normal and (iv) superconducting states. Sub-task (i) was solved in work [37] devoted to the theoretical consideration of the normal HTT phase properties within the Hubbard model. Since spectral weight distribution is correctly reproduced within the Hubbard model proper description of the DOS effects should be performed using this model. It was shown in [37] that the behavior of the exchange interaction parameter and DOS with the same change in the CuO_2 lattice parameter a and b (the lattice strain in the tetragonal phase) has a different character. The exchange interaction parameter decreases with the CuO_2 lattice parameter increasing due to the decrease of intercell hopping integrals which determine the effective superexchange interaction. DOS increases with the CuO_2 lattice parameter increasing since the conductivity and valence bandwidths decrease when the Cu-O distance grows, while the number of states remains constant. Thus it is unclear how T_c will behave eventually with the Cu-O distance changing in the tetragonal phase. One of the goals of our present work which is a continuation of [37] is to answer this question by studying the effect of the same change in the CuO_2 lattice parameter a and b on the concentration T_c dependence in the superconducting HTT phase (sub-task (ii)).

A separate issue to be clarified is the role of DOS in the formation of the observed concentration and the Cu-O distance dependences of T_c, whether the optimal doping is determined by the hole concentration at which the chemical potential falls on the van Hove singularity in the density of states. T_c in cuprates has a concentration dependence with the form of a dome with one maximum at a hole concentration of $x = 0.16$. In the same concentration range, a flat band was observed in the dispersion obtained by ARPES [38, 39] at the point $(\pi, 0)$, the presence of this flat band leads to a peak in DOS. The peaks in the DOS at a hole concentration coinciding with the optimal doping were obtained in frameworks of theoretical calculations within the t-t'-t"'-J* model taking into account the exchange pairing mechanism in [40]. Although saddle points that bring to crucial van Hove singularity are located at points of the Brillouin zone boundaries apart from $(\pi, 0)$, the same type of saddle point at $k = (\pi, 0)$ as in ARPES is located much deeper in the valence band and chemical potential coincides with corresponding van Hove singularity at heavily overdoped compounds. It is clear from the work [40] that the topology of the dispersion surface significantly affects the concentration dependence of T_c of cuprates. Inhomogeneous distribution of the spectral weight over the Fermi surface was found by ARPES [41–47] to form arcs instead of closed pockets and was reproduced within the framework of the Hubbard model by different approaches in the regime of strong electron correlations [37, 48–52]. The inhomogeneous spectral weight corrects the DOS, and it is necessary to calculate the concentration dependence of T_c precisely taking into account the pseudogap states for the Hubbard model. Significant change of the dispersion topology is assumed in the orthorhombic phase due to the presence of two different hopping integrals along with two directions of the CuO_2 plane. The LTO phase of cuprates has hardly been studied theoretically. The mechanism of the influence of orthorhombic distortion on T_c is not clear.

The present paper is aimed at solving sub-tasks (ii), (iii), and (iv). The main part of this work is devoted to the theoretical investigation of the influence of orthorhombic distortion accompanied by the average Cu-O distance variation on the electronic structure in the normal state and the concentration T_c dependence in the superconducting state of cuprates in the LTO phase. In the orthorhombic phase, the z-axis of CuO_6 octahedra is rotated at some angle, the angle between x and y axes in the CuO_2 plane deviates from 90 degrees, CuO_2 lattice parameters $b > a$. The main effect of orthorhombic distortion is from the difference of the lattice parameters a and b which is expressed by orthorhombicity factor $\delta b/a = (b-a)/a$ since it significantly influences the electronic structure in the CuO_2 plane and the value of exchange interaction. Also, we will compare the effects of average Cu-O distance influence on properties of cuprates in the orthorhombic phase and previously considered tetragonal phase [37]. We model different cuprate compounds by a layer of the CuO_6 octahedra with corresponding Cu-O distances. Variation of CuO_2 lattice parameters in tetragonal and orthorhombic phases is simulated by the isotropic and uniaxial stress of the CuO_2 layer, respectively. Joint variation of average Cu-O distance and orthorhombic distortion among different cuprates is modeled by elongation (shortening) of lattice parameter a with fixed elongated parameter b. Adequate strong electronic correlations (SEC) treatment is reached by applying the generalized tight-binding method (GTB method) [53, 54] which is a cluster perturbation theory in terms of Hubbard operators.

The paper includes six sections. Section 2 describes the system to be studied, the Hamiltonian of charge carriers in this system that is obtained from the LDA calculations and briefly reports the method for calculating the electronic structure and superconducting properties. In Section 3 we will discuss the effects of orthorhombic distortion on the band structure, Fermi contour, and DOS of quasiparticle excitations. Section 4 contains the effects of joint variation of orthorhombicity factor and average Cu-O distance on superconducting properties in the orthorhombic phase. Section 5 contains effects of CuO_2 lattice parameter variation on concentration dependence of T_c in the tetragonal phase. In section 6 the main results are summarized.

2 Hamiltonian of Five-band p-d Model and Method for Calculating Electronic Structure and Superconducting Properties

The electronic system of the layer of CuO_6 octahedra is described within the multiband p-d model in the basis of copper $d_{x^2-y^2}$- , $d_{3z^2-r^2}$-orbitals, oxygen planar p_x- , p_y -orbitals, and apical p_z-orbitals. Further orbital $d_{x^2-y^2}$ will be denoted by d_x and $d_{3z^2-r^2}$ - by d_z. Hamiltonian of the p-d model with taking into account only nearest neighbor hoppings takes the form:

$$
\begin{aligned}
H = & \sum_{\lambda f\sigma} \varepsilon_{d\lambda}(\delta b/a) n^{\lambda}_{df\sigma} + \sum_{\lambda g\sigma} \varepsilon_{p\lambda}(\delta b/a) n^{\lambda}_{pf\sigma} + \\
& \sum_{\langle fg\rangle\sigma} \left[t^{\lambda\lambda'}_{dp} d^{\dagger}_{\lambda f\sigma} p_{\lambda' g\sigma} + t^{\lambda\lambda'}_{pp} p^{\dagger}_{\lambda f\sigma} p_{\lambda' g\sigma} + h.c. \right] + \\
& \sum_{\lambda f} U_d n^{\lambda}_{df\uparrow} n^{\lambda}_{df\downarrow} + \sum_{\lambda g} U_p n^{\lambda}_{pg\uparrow} n^{\lambda}_{pg\downarrow} + \\
& \sum_{\langle fg\rangle} \sum_{\lambda\lambda'\sigma\sigma'} V_{pd} n^{\lambda}_{df\sigma} n^{\lambda'}_{pg\sigma'} + \sum_{\langle fg\rangle} \sum_{\lambda\lambda'\sigma\sigma'} V_{pp} n^{\lambda}_{pf\sigma} n^{\lambda'}_{pg\sigma'} + \\
& \sum_{f\sigma\sigma'} J_d n^{x}_{df\sigma} n^{z}_{df\sigma'}
\end{aligned}
\tag{1}
$$

Here $n^{d}_{\lambda f\sigma} = d^{\dagger}_{\lambda f\sigma} d_{\lambda f\sigma}$, $n^{\lambda}_{pg\sigma} = p^{\dagger}_{\lambda g\sigma} p_{\lambda g\sigma}$ are particle number operators. Indexes f, g indicate the position of atom on which given orbital is located, indexes σ, σ' are the spin projection of hole on this orbital, indexes λ, λ' denote the type of orbital, $\lambda = x, z$ is for d-orbitals and $\lambda, \lambda' = x, y, z$ for p-orbitals. Angle bracket $\langle fg\rangle$ denotes nearest-neighbor hoppings. Here $\varepsilon_{d\lambda} = \varepsilon_{dx}, \varepsilon_{dz}$ are onsite energies of the hole on d_x-, d_z -orbitals of the copper atom and $\varepsilon_{p\lambda} = \varepsilon_{px}, \varepsilon_{py}, \varepsilon_{pz}$ are onsite energies on p_x-, p_y-orbitals of the planar oxygen atom, p_z -orbital of the apical oxygen atom, respectively, $t^{\lambda\lambda'}_{dp}$ is hopping parameter between atomic orbital d_λ of copper and orbital $p_{\lambda'}$ of oxygen, $t^{\lambda\lambda'}_{pp}$ is oxygen–oxygen hopping between oxygen orbitals p_λ and $p_{\lambda'}$. Hamiltonian (1) describes both tetragonal and orthorhombic phases. All Hamiltonian parameters for the tetragonal phase have been calculated within the LDA+GTB approach [55].

Hopping integrals along the x-axis $t^{\lambda x}_{dp}$, $t^{x\lambda'}_{pp}$ and along the y-axis $t^{\lambda y}_{dp}$, $t^{y\lambda'}_{pp}$ are equal in the tetragonal phase and differ in the orthorhombic phase. Variation of average Cu-O distance in different compounds in the orthorhombic phase is accompanied by a variation of orthorhombic distortion. Variation of lattice parameter a with fixed CuO_2 lattice parameter b at distorted value for which $\delta b/b_0 = (b-b_0)/b_0 = 4.15\,\%$ regulates joint variation of average Cu-O distance and orthorhombicity factor $\delta b/a = (b-a)/a$. It is assumed that a variation of the CuO_2 lattice parameter a in the orthorhombic phase changes only those parameters of Hamiltonian that react most strongly to a change of Cu-O distance along the x-axis. We consider the dependence of hopping parameters t^{xx}_{dp}, t^{zx}_{dp} and t^{xz}_{pp} on CuO_2 lattice parameter a (Table 1). The dependence of these parameters on Cu-O distance along the x-axis is taken the same as the dependence of analogous parameters on the isotropic strain of the CuO_2 lattice in the tetragonal phase [37]. We consider that onsite energies $\varepsilon_{dx}, \varepsilon_{dz}, \varepsilon_{p_x}, \varepsilon_{p_y}, \varepsilon_{p_z}$ and hopping parameters t^{zz}_{dp}, t^{xy}_{pp}, t^{zy}_{dp}, t^{yz}_{pp} do not depend on the CuO_2 lattice parameter a and their magnitudes are fixed at values for isotropic 4.15 % strain

Table 1 Values of hopping parameters (in eV) t_{dp}^{xx}, t_{dp}^{zx} and t_{pp}^{xz} at different orthorhombicity factor $\delta b/a$ which is changed by shortening of a parameter (along the x-axis) in the CuO_2 plane, b parameter (along the y-axis) is fixed. Variation of these hopping parameters with the change of CuO_2 lattice parameter a is taken the same as variation of these parameters with the identical change of CuO_2 lattice parameters a and b in the tetragonal phase [37]

$\delta b/a$	t_{dp}^{xx}	t_{dp}^{zx}	t_{dp}^{xz}
0 %	1.201	0.570	0.462
1.65 %	1.280	0.549	0.443
3.65 %	1.379	0.526	0.415
4.15 %	1.403	0.523	0.403

in tetragonal phase [37]. Relations between hopping parameters along x and y axis in the orthorhombic phase are:

$$t_{dp}^{xy} = \kappa t_{dp}^{xx}, t_{dp}^{zy} = \kappa' t_{dp}^{zx}, t_{pp}^{yz} = \beta t_{pp}^{xz} \tag{2}$$

In the tetragonal phase, coefficients κ, κ', β are equal to one.

U_d, U_p are parameters of intraatomic Coulomb interaction of holes on copper and oxygen atoms, respectively. V_{pd} and V_{pp} are the interatomic Coulomb interaction of holes on copper and oxygen atoms and on neighbor oxygen atoms, respectively. J_d is the parameter of exchange interaction of holes on d_x- and d_z-orbitals. The values of Coulomb parameters (in eV) are:

$$U_d = 9, U_p = 4, V_{pd} = 1.5, V_{pp} = 1, J_d = 1 \tag{3}$$

In the tetragonal phase, onsite energies and hopping parameters at different CuO_2 lattice strains $\delta a/a_0 = (a - a_0)/a_0$, where $a_0 = b_0$ and $a = b$ are lattice parameters of undistorted and distorted La_2CuO_4, respectively, are taken from the work [37].

The electronic structure of cuprates as systems with strong electronic correlations can be correctly described in the terms of the Hubbard fermions [57] using the GTB method [53]. The scheme of the GTB method has been described in detail in many works as applied to cuprates [53–56]. In this paper, we have generalized the GTB method to describe cuprates with orthorhombic distortion. The peculiarities of the GTB method implementation associated with different values of the CuO_2 lattice parameters a and b are given in Appendices 2, 3, and 4. Appendix 2 describes the orthogonalization procedure for oxygen atomic orbitals with the formation of a basis of molecular orbitals localized within one cluster in the form of the CuO_6 octahedron. Also, Appendix 2 contains the five-band p-d model Hamiltonian on the basis of the original copper orbitals and the new molecular oxygen orbitals. The structure of the orthorhombic cluster eigenstates on which Hubbard fermions are constructed is given in Appendix 3. Hubbard fermion (pq) is the quasiparticle excitation between cluster eigenstates $|q\rangle$ and $|p\rangle$ which is described by Hubbard operators $X_f^{pq} = |p\rangle\langle q|$. We will use the same basis of quasiparticle excitations, Hamiltonian of two-band Hubbard model for quasiparticle excitations as in [58] but in the orthorhombic phase, the intercluster quasiparticle hopping parameters in the Hubbard model have different values along the x and y crystallographic axis (Appendix 4). The electronic structure of Hubbard fermions is obtained using the equation of motion method for matrix two times retarded Green's function within generalized mean-field approximation also as in [37, 58]. Dependences of superconducting transition temperature T_c on CuO_2 lattice strain and orthorhombic distortion at different doping are calculated within the exchange mechanism of pairing inside the valence band in the spirit of Plakida's work [58]. In the tetragonal phase, we consider the only superconducting pairing of d-symmetry with the gap $\Delta_{\mathbf{k}} = \Delta_d(\cos(k_x) - \cos(k_y))$. In the orthorhombic phase, the superconducting gap may have an additional s-symmetry contribution by symmetry reasons [59–61] and as follows from experimental data [62, 63]. Therefore, we will look for the superconducting gap in the form of the sum of d-symmetry and extended s*-symmetry: $\Delta_{\mathbf{k}} = \Delta_d(\cos(k_x) - \cos(k_y)) + \Delta_{s*}(\cos(k_x) + \cos(k_y))$. To obtain T_c, we consider the system of equations for d- and s*-components of the superconducting gap as the eigenvalue task in the basis of states $\{\Delta_d + \Delta_{s*}, \Delta_{s*} - \Delta_d\}$ with fixed eigenvalue $\lambda = 1$ according to Val'kov's and Dzebisashvili's works [64, 65].

3 Electronic Structure of Quasiparticle Excitations in the System with Orthorhombic Distortion

The band structure of quasiparticle excitations within the effective Hubbard model is two bands with inhomogeneous distribution of spectral weight divided by the gap of 2 eV. The valence band maxima are at k-points $(\pi/2, \pi/2)$, $(3\pi/2, \pi/2)$, $(\pi/2, 3\pi/2)$, $(3\pi/2, 3\pi/2)$. The bottom of the conductivity band is at k-points $(\pi, 0)$ and $(0, \pi)$ in the tetragonal phase and there is only one minimum at the point $(\pi, 0)$ in the orthorhombic phase. In the orthorhombic phase, the dispersion surface is non-symmetrical relative to nodal direction due to the difference of intercluster hopping parameters along the x- and y-axis. Band structure along boundaries of a quarter of Brillouin zone is shown in Fig. 1. The asymmetry can be seen in the band structure along boundaries $(\pi, 0)$-(π, π) and $(0, \pi)$-(π, π) (Fig. 1a-f). An increase in the number of doped holes lowers the chemical potential level inside the valence band. At low doping, the Fermi contour consists of the four small hole pockets around

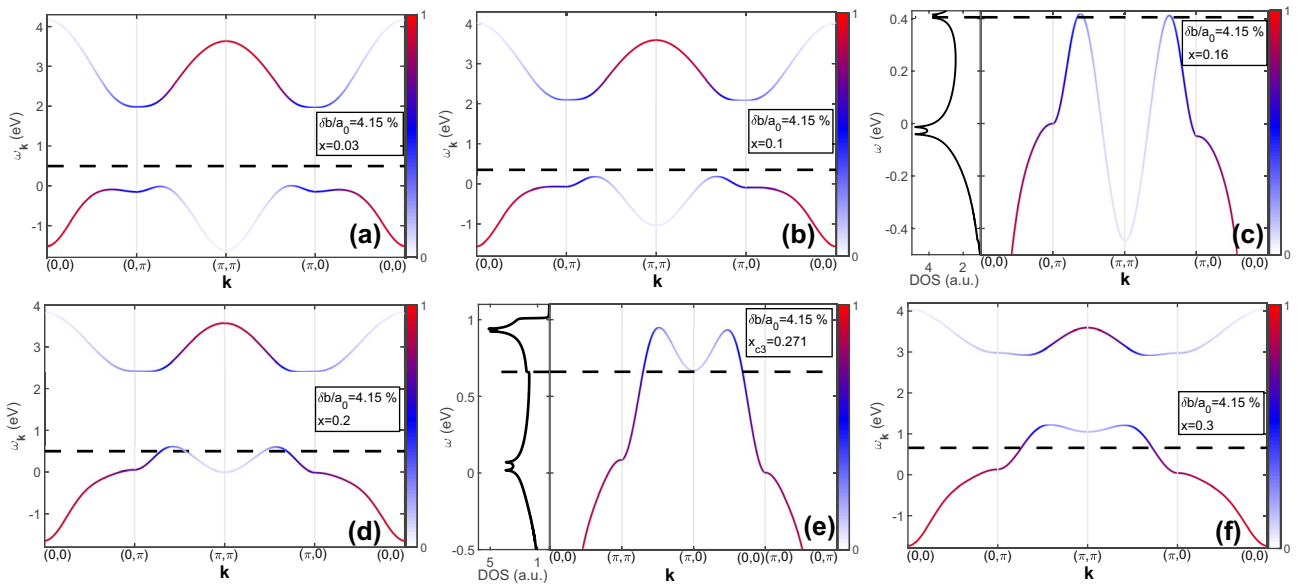

Fig. 1 (Color online) The reconstruction of band structure with doping at orthorhombicity factor $\delta b/a = 4.15\%$. The band structure is builded in directions of boundaries of the quarter Brillouin zone. It is seen that dispersion is non-symmetrical relative to nodal direction. In the left panels of subfigures **(c)** and **(e)**, density of states of quasiparticle excitations at second and third critical doping $x_{c2} = 0.161$ and $x_{c3} = 0.271$ are depicted. The color of each point of dispersion characterizes the spectral weight of electrons. Dashed line indicates the Fermi level

k-points $(\pi/2, \pi/2), (3\pi/2, 3\pi/2), (3\pi/2, \pi/2), (\pi/2, 3\pi/2)$ (Fig. 2a). These pockets are asymmetric with respect to the directions $(0, 0)$-$(2\pi, 2\pi)$ and $(2\pi, 0)$-$(0, 2\pi)$. These pockets grow with hole concentration increasing. Because of dispersion, surface asymmetry relative to nodal directions chemical potential reaches a local maximum of the quasiparticle energy in the direction $(0, \pi)$-$(2\pi, \pi)$ at smaller doping than in the direction $(\pi, 0)$-$(\pi, 2\pi)$ (Fig. 1c). Hole pockets touch each other at k-point of direction $(0, \pi)$-$(2\pi, \pi)$ at first critical concentration x_{c1}, where four pockets transform into two hole pockets of complex form by the Lifshitz transition (Fig. 2b). At the concentration $x_{c1} = 0.155$, chemical potential falls on one of the two van Hove singularities in the density of states (DOS). At the second critical doping

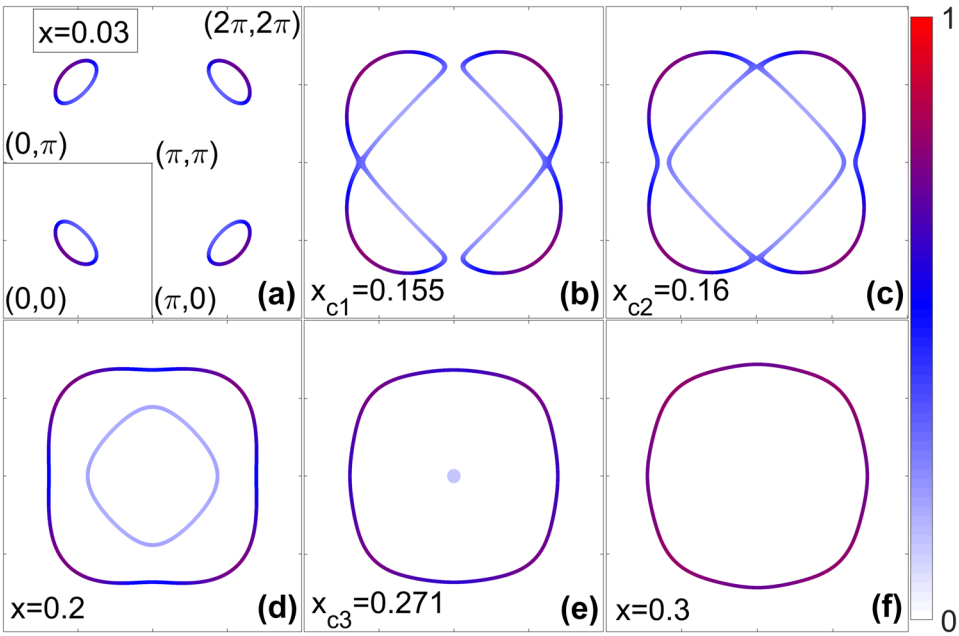

Fig. 2 (Color online) The reconstruction of Fermi contour with doping at orthorhombic distortion $\delta b/a = 4.15\%$. Change of Fermi contour topology occurs at three dopings x_{c1}, x_{c2} and x_{c3}. The color of each point of dispersion characterizes the spectral intensity of electrons

$x_{c2} = 0.16$ these two pockets touch each other at k-point of direction $(\pi, 0)$-$(\pi, 2\pi)$ (Fig. 2c), Fermi contour takes the form of one large hole contour and large electron contour, chemical potential falls on the second of the two van Hove singularities in DOS (Fig. 1c, left panel). Further growth of hole concentration leads to electron contour decreasing (Fig. 2d). At the third critical concentration $x_{c3} = 0.271$, chemical potential falls into a step-like singularity in DOS (Fig. 1e, left panel) which results from the local minimum at point (π, π) (Fig. 1e, right panel). As the chemical potential drops below the local minimum at point (π, π) (Fig. 1f), the electron contour vanishes (Fig. 2e). Above hole concentrations x_{c2} in the tetragonal phase and x_{c3} in the orthorhombic phase the normal Fermi liquid state with the uniform distribution of the spectral weight over the Fermi contour is restored (Fig. 2f).

4 Superconducting Properties of the System with Orthorhombic Distortion

The dependence of T_c on the orthorhombic distortion is calculated in the doping interval x from 0.03 to 0.3. The concentration dependence of T_c is calculated at orthorhombicity factors $\delta b/a = 0,\ 1.65,\ 3.65,\ 4.15\%$. Growth of $\delta b/a$ from 0 to 4.15% is modeled by the decrease of CuO_2 lattice parameter a from elongated value $a = b$ $(\delta b/b_0 = \delta a/a_0 = 4.15\%)$ to undistorted lattice parameter $a = a_0(\delta b/b_0 = 4.15\%, \delta a/a_0 = 0\%)$ with fixed elongated lattice parameter b. Such variation allows to jointly change the orthorhombicity factor and the average Cu-O distance for theoretical calculations in the same manner as these parameters change in behavior of experimental T_c maxima in different cuprates as a function of various average Cu-O distances in the LTO region [34]: the shorter average Cu-O distance the stronger orthorhombic distortion. The exchange interaction between nearest neighbors differs along the x- and y-axes, for example, $J^x_{01} = 0.673$ eV and $J^y_{01} = 0.655$ eV at the orthorhombic distortion $\delta b/a = 4.15\%$. Exchange parameters J^x_{01} and J^y_{01} grow with CuO_2 lattice parameter a decrease (orthorhombic distortion increasing). The concentration dependence of T_c is a dome with one maximum (Fig. 3a) which is in the region of the two-hole critical concentrations x_{c1} and x_{c2} at which the chemical potential falls on the van Hove singularities. The CuO_2 lattice parameter a increase (orthorhombic distortion decreasing) leads to T_c decreasing at all hole concentrations and also shifts the value of the optimal doping to larger values (Fig. 3a). The most significant T_c decrease is found in the region of optimal doping, in the underdoped and overdoped compounds the difference of T_c for various orthorhombic distortions is smaller. We varied the exchange interaction value to clarify its role on the concentration dependence of T_c. The artificial J

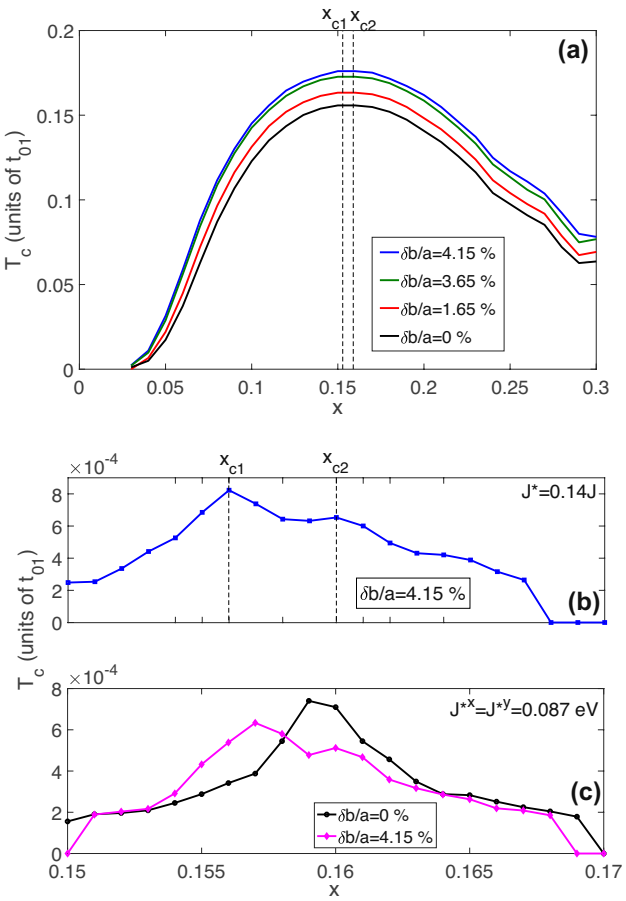

Fig. 3 (Color online) The dependence of superconducting dome on orthorhombic distortion. Dotted lines denote two critical concentrations x_{c1} and x_{c2}. **(b)** Two T_c maxima resulted from two van Hove singularities in the system with orthorhombic distortion and partially suppressed exchange parameter J. **(c)** Regions of the concentration dependence of T_c near optimal doping with and without orthorhombic distortion at strongly suppressed exchange parameter J. The T_c maximum grows with average Cu-O distance increasing (orthorhombic distortion decreasing) if the effect of DOS on T_c prevails over the effect of exchange parameter

decrease results in T_c decreasing at all concentrations. There is only one maximum of the superconducting dome up to the value of variable exchange interaction constant $J^* = 0.2J$ $(J^{*x}_{01} = 0.135\,\text{eV}$ and $J^{*y}_{01} = 0.131\,\text{eV})$. Two maxima begin to appear only at $J^* = 0.15J (J^{*x}_{01} = 0.101$ eV and $J^{*y}_{01} = 0.098$ eV). These maxima appear at critical concentrations x_{c1} and x_{c2} (Fig. 3b).

To find out the pure effect of the DOS on superconducting temperature we make some artificial speculations. We make constants J^x_{01} and J^y_{01} equal to each other in the orthorhombic phase. We fix J^x_{01} and J^y_{01} on the value of exchange interaction for elongated Cu-O bonds $\delta b/b_0 = \delta a/a_0 = 4.15\%$, $\delta b/a = 0\%$. Also, we reduce the value of $J^x_{01}(J^y_{01})$ by 14% of the original constant so $J^{*x}_{01} = J^{*y}_{01} = 0.14J_{01}\left(\delta a/a_0 = 4.15\%\right) = 0.087$ eV. Due to

these assumptions, influence of orthorhombic distortion on T_c through the exchange interaction constant is suppressed and only influence through the DOS remains. In this case, the T_c maximum for uniformly distorted CuO_2 lattice ($\delta b/b_0 = \delta a/a_0 = 4.15\%, \delta b/a = 0\%$) is higher than for orthorhombically distorted CuO_2 lattice ($\delta b/a = 4.15\%$)(Fig. 3c). Under these assumptions, the average Cu-O distance increase results in the growth of T_c. However such behavior disappears at $J^x_{01}(J^y_{01})$ increasing and the effect of DOS becomes invisible. Since the dependence of T_c on the CuO_2 lattice parameter a is determined by dependence of J^x_{01} and J^y_{01} on a, the effect of the exchange parameter on T_c is predominant in comparison with the influence of the density of states.

5 Influence of CuO_2 Lattice Parameter Change on the Concentration Dependence of T_c in the Tetragonal Phase

The previous section was devoted to the influence of the orthorhombic distortion change accompanied by the average Cu-O distance variation on the dependence of T_c for compounds in the LTO phase. In this section, we consider the dependence of T_c on the average Cu-O distance caused by the same change in the CuO_2 lattice parameters a and b for compounds in the HTT phase. Electronic structure, superconducting gap, and T_c are calculated using formulas for the orthorhombic phase under the condition that the coefficients κ, κ', β are equal to one. The concentration dependence of T_c in the doping interval x from 0.03 to 0.3 is a dome (Fig. 4) with a maximum at doping $x = 0.16$ (Fig. 4, dotted line) that coincides with the hole concentration at which the chemical potential falls on the van Hove singularity. The CuO_2

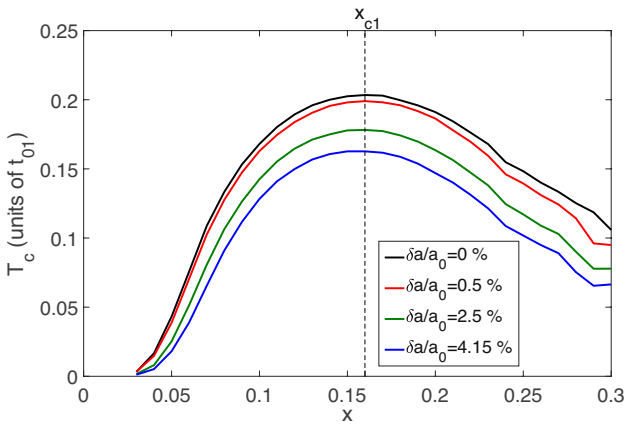

Fig. 4 (Color online) The dependence of superconducting dome on CuO_2 lattice parameter $a = b$ in the tetragonal phase of cuprates. The dotted line denotes the critical concentration of the first quantum phase transition x_{c1} at $\delta a/a_0 = 0$

lattice parameter increase ($\delta a\ a_0$ increasing) results in the T_c decreasing at all hole concentrations. Also, there is a slight shift of the optimal doping value to a smaller value with the CuO_2 lattice parameter increasing since CuO_2 lattice elongation leads to the weak decrease of x_{c1} according to work [37]. It is clear that the dependence of T_c on CuO_2 lattice parameter value is caused by the behavior of the exchange constant J on parameter a but not DOS which decreases with a increasing [37].

6 Conclusions

In the tetragonal phase CuO_2 lattice parameter increasing leads to T_c decreasing at all doped hole concentrations in the range from 0.03 to 0.3. This calculated dependence of the maximum T_c on the CuO_2 lattice parameter reproduces the behavior of the maximum T_c values in various cuprates as a function of the Cu-O distance. This may indicate that the Cu-O distance in the CuO_2 layer, a common structural element of cuprates, is the parameter that controls T_c in these compounds. Mechanism of Cu-O distance influence on T_c is a variation of the exchange interaction constant with Cu-O bonds shortening (elongation). The optimal doping is determined by the hole concentration x_{c1} at which the chemical potential falls on the van Hove singularity.

The main effect of orthorhombic distortion on electronic structure is asymmetry of dispersion surface and Fermi contour of quasiparticle excitations relative to nodal direction. Saddle points of dispersion surface on the two boundaries of Brillouin zone have different energy and therefore each van Hove singularity that DOS had in the tetragonal phase splits into two peaks in the orthorhombic phase. Transformation of the Fermi contour from four small hole pockets into a large hole and large electron contours with doping goes through two stages at concentrations x_{c1} and x_{c2}. Chemical potential at x_{c1} and x_{c2} falls on each of the two van Hove singularities. Elongation of average Cu-O distance and orthorhombicity factor decreasing which are modeled by CuO_2 lattice parameter a increasing with fixed elongated parameter b result in maximum T_c decreasing in the orthorhombic phase. The presence of two van Hove singularities in DOS is manifested at small J in the form of two peaks in concentration dependence of T_c at those concentrations x_{c1} and x_{c2} when chemical potential falls on these singularities.

Calculated dependence of T_c maximum on average Cu-O distance in orthorhombic phase doesn't reproduce the behavior of the experimental T_c maximum with the growth of average Cu-O distance in different cuprates. Mechanism of J decreasing with Cu-O bonds elongation that allows describing the dependence of experimental T_c maxima on Cu-O distance in the tetragonal phase works against such dependence in the orthorhombic phase. To separate the effect of

DOS changes on T_c with joint average Cu-O bond elongation and orthorhombicity factor decreasing one may consider the exchange interaction J to have the suppressed value for all considered systems and to be independent on lattice distortions. It looks like that such a simplified approach is in agreement with the behavior of experimental values of T_c maximum on average Cu-O distance in the orthorhombic phase. However, this DOS mechanism works only when the mechanism of J renormalization with Cu-O bond variation is suppressed. Apparently, to describe the observed dependence in the LTO region, it is necessary to take into account more complex effects of orthorhombic distortion. Charge and orbital ordering formed from polaronic stripes were found in Bi2212 [66, 67] and LSCO [68–70] compounds. The presence of polaronic lattice distortions indicates strong electron-phonon coupling in cuprates. Variation of the Cu-O bond lengths and O-Cu-O angles in the orthorhombically distorted system induces elastic strain field which changes electron-lattice coupling constant. As a result of the strong electron-phonon coupling, electronic structure and DOS will also change. DOS renormalization, a renormalization of the magnitude of the electron-phonon mechanism of pairing or both can cause variation of T_c. Besides charge ordering itself which is observed in the orthorhombic phase (for example in underdoped LSCO [71]) also can significantly change electronic structure and influence on superconducting state through the DOS.

Appendix

Orthogonalization Procedure of Atomic Oxygen Orbitals in CuO_6 Octahedron

We choose the CuO_6 octahedron as a cluster. Since each in-plane oxygen atom simultaneously belongs to two clusters it is necessary to produce orthogonalization of oxygen orbitals. Orthogonalization procedure for tetragonal lattice is described in work [72], the molecular orbitals b_f and a_f in the cluster f are introduced instead of the atomic oxygen orbitals p_{xh} and p_{yh} at sites h using transformation in the k-space:

$$\begin{aligned} b_{\mathbf{k}} &= -\frac{i}{\mu_{\mathbf{k}}}\left(s_{x\mathbf{k}}p_{x,\mathbf{k}} - s_{y\mathbf{k}}p_{y\mathbf{k}}\right) \\ a_{\mathbf{k}} &= -\frac{i}{\mu_{\mathbf{k}}}\left(s_{y\mathbf{k}}p_{x,\mathbf{k}} + s_{x\mathbf{k}}p_{y\mathbf{k}}\right) \end{aligned} \tag{4}$$

where $s_{kx} = \sin\left(k_x a\,2\right)$, $s_{ky} = \sin\left(k_y b\,2\right)$, $\mu_{\mathbf{k}} = \sqrt{s_{kx}^2 + s_{ky}^2}$. Molecular orbitals in the different unit cells are orthogonal to each other. Also, bonding and antibonding orbitals of apical oxygens were introduced

$$\begin{aligned} p^b_{zf\sigma} &= \frac{1}{\sqrt{2}}\left(p_{z(f+c')\sigma} - p_{z(f-c')\sigma}\right) \\ p^a_{zf\sigma} &= \frac{1}{\sqrt{2}}\left(p_{z(f+c')\sigma} + p_{z(f-c')\sigma}\right) \end{aligned} \tag{5}$$

Remain basis orbitals hybridize with only bonding orbital of apical oxygen. Antibonding orbital doesn't hybridize with nearest orbitals, lies higher in energy, and doesn't participate in the formation of low-energy excitations. Therefore further we will consider only bonding orbital $p_{zf} = p^b_{zf}$. When we take into account transformations (2),(4),(5) Hamiltonian of five-band p-d model for tetragonal and orthorhombic phases takes the general form:

$$\begin{aligned} H = &\sum_{f\sigma}\left(\varepsilon_{d\lambda}n^{\lambda}_{df\sigma} + \varepsilon_b n^b_{f\sigma} + \varepsilon_a n^a_{f\sigma} + \varepsilon_{pz}n^{pz}_{f\sigma}\right) + \\ &\sum_{fg\sigma} 2t^{xx}_{dp}\Big[-\left(\mu_{fg} + \rho_{fg}(\kappa-1)\right)d^{\dagger}_{xf\sigma}b_{g\sigma} + \\ &\lambda_{fg}(1-\kappa)d^{\dagger}_{xf\sigma}a_{g\sigma} + h.c.\Big] + \\ &\sum_{fg\sigma} 2t^{xx}_{dp}\Big[-\left(\mu_{fg} + \rho_{fg}(\kappa-1)\right)d^{\dagger}_{xf\sigma}b_{g\sigma} + \\ &\lambda_{fg}(1-\kappa)d^{\dagger}_{xf\sigma}a_{g\sigma} + h.c.\Big] + \\ &\sum_{fg\sigma} 2t^{zx}_{dp}\Big[\left(\mu_{fg} - \rho_{fg}\left(1+\kappa'\right)\right)d^{\dagger}_{zf\sigma}b_{g\sigma} - \\ &-\lambda_{fg}\left(1+\kappa'\right)d^{\dagger}_{zf\sigma}a_{g\sigma} + h.c.\Big] - \\ &\sum_{fg\sigma} 2t^{xy}_{pp}\Big[\nu_{fg}b^{\dagger}_{f\sigma}b_{g\sigma} - \nu_{fg}a^{\dagger}_{f\sigma}a_{g\sigma} + \\ &\left(\chi_{fg}b^{\dagger}_{f\sigma}a_{g\sigma} + h.c.\right)\Big] - \\ &\sum_{f\sigma}\sqrt{2}t^{zz}_{dp}\left[d^{\dagger}_{zf\sigma}p^b_{zf\sigma} + h.c.\right] + \\ &\sum_{fg\sigma} 2\sqrt{2}t^{xz}_{pp}\Big[\left(\mu_{fg} - \rho_{fg}(\beta+1)\right)b^{\dagger}_{f\sigma}p_{zg\sigma} - \\ &\lambda_{fg}(1+\beta)a^{\dagger}_{f\sigma}p_{zg\sigma} + h.c.\Big] + \\ &\sum_{\lambda\lambda' f}\left(U_d n^{\lambda}_{df\uparrow}n^{\lambda'}_{df\downarrow} + U_p n^{z}_{pf\uparrow}n^{z}_{pf\downarrow}\right) + \\ &\sum_{f\sigma\sigma'} J_d n^{x}_{df\sigma}n^{z}_{df\sigma'} + \sum_{fg\lambda\sigma\sigma'} V_{pd}n^{\lambda}_{df\sigma}n^{z}_{pg\sigma'} + \\ &\sum_{fghl}\sum_{\lambda_1\lambda_2\lambda_3\lambda_4} U_p\Psi_{fghl}P^{\dagger}_{\lambda_1 f\uparrow}P_{\lambda_2 g\uparrow}P^{\dagger}_{\lambda_3 h\downarrow}P_{\lambda_4 l\downarrow} + \\ &\sum_{fh\sigma\sigma'}\sum_{\lambda_1\lambda_2=b,a} V_{pd}\Phi_{fgh}n^{d}_{\lambda f\sigma}P^{\dagger}_{\lambda_1 g\sigma'}P_{\lambda_2 h\sigma'} \end{aligned} \tag{6}$$

Here $n^b_{f\sigma} = b^\dagger_{f\sigma} b_{f\sigma}$, $n^a_{f\sigma} = a^\dagger_{f\sigma} a_{f\sigma}$. The operator $P_{\lambda g\sigma}$ annihilates the hole on one of the molecular oxygen orbitals $b_{g\sigma}$ and $a_{g\sigma}$: $P_{\lambda g\sigma} = \{P_{bg\sigma}, P_{ag\sigma}\} = \{b_{g\sigma}, a_{g\sigma}\}$. Definitions of the structural factors ν_{fg}, χ_{fg} [54, 73], λ_{fg}, ρ_{fg} in momentum space are:

$$\begin{aligned} \nu_{\mathbf{k}} &= \frac{4 s^2_{kx} s^2_{ky}}{\mu^2_{\mathbf{k}}}, \chi_{\mathbf{k}} = \frac{2 s_{kx} s_{ky} \left(s^2_{kx} - s^2_{ky} \right)}{\mu^2_{\mathbf{k}}}, \\ \lambda_{\mathbf{k}} &= \frac{s_{kx} s_{ky}}{\mu_{\mathbf{k}}}, \rho_{\mathbf{k}} = \frac{s^2_{kx}}{\mu_{\mathbf{k}}} \end{aligned} \tag{7}$$

Dependences of these structural factors for a couple of sites f and g from the distance between them and their orientation are given in Table 2.

The magnitude of coefficients Φ_{fgh} and Ψ_{fghl} rapidly decreases with distance therefore we will take into account only Coulomb interactions within each cluster $\Phi_{000} = 0.918$ and $\Psi_{0000} = 0.2109$ [54].

Cluster Eigenstates

The exact diagonalization of the CuO_6 octahedron gives its eigenstates in the 0-, 1- 2-hole sectors of Hilbert space. Single-hole eigenstates of the CuO_4 cluster without orthorhombic distortion are classified into states of b_{1g} and a_{1g}. The ground state in the tetragonal phase is the state of b_{1g} symmetry $|\sigma\rangle = c^{dx}_0 |d_{x\sigma}\rangle + c^b_0 |b_\sigma\rangle$. States of a_{1g} symmetry $c^{dz}_i |d_{z\sigma}\rangle + c^a_i |a_\sigma\rangle + c^{pz}_i |p_{z\sigma}\rangle$ are higher in energy. States of a_{1g} symmetry mix in states of b_{1g} symmetry in the CuO_4 cluster with orthorhombic distortion, the ground state is $|\sigma\rangle = c^{dx}_0 |d_{x\sigma}\rangle + c^b_0 |b_\sigma\rangle + c^{dz}_0 |d_{z\sigma}\rangle + c^a_0 |a_\sigma\rangle + c^{pz}_0 |p_{z\sigma}\rangle$. Probability amplitudes of basis orbitals in the ground state for orthorhombic distortion δb $a = 4.15\%$ are

c^{dx}_0	c^b_0	c^{dz}_0	c^a_0	c^{pz}_0
0.6946	0.7176	0.0287	-0.0099	0.0402

Two-hole ground eigenstate in the tetragonal phase is the A_1 singlet formed by productions of the states of b_{1g} symmetry $|S\rangle = L^{dd}_0 \left(d_{x\downarrow} b_\uparrow - d_{x\uparrow} b_\downarrow \right) + L^{dd}_0 |d_{x\downarrow} d_{x\uparrow}\rangle + L^{bb}_0 |b_\downarrow b_\uparrow\rangle$. In the orthorhombic phase the ground state is singlet that includes productions of the single hole states of b_{1g} symmetry, productions of orbitals of a_{1g} symmetry, and production of b_{1g} and a_{1g} orbitals:

$$\begin{aligned} |S\rangle = \; & L^{dxdx}_0 \left(d_{x\downarrow} b_\uparrow - d_{x\uparrow} b_\downarrow \right) + L^{dxdx}_0 |d_{x\downarrow} d_{x\uparrow}\rangle + L^{bb}_0 |b_\downarrow b_\uparrow\rangle + \\ & L^{dza}_0 \left(d_{z\downarrow} a_\uparrow - d_{z\uparrow} a_\downarrow \right) + L^{dzdz}_0 |d_{z\downarrow} d_{z\uparrow}\rangle + L^{aa}_0 |a_\downarrow a_\uparrow\rangle + \\ & L^{dzpz}_0 \left(d_{z\downarrow} p_{z\uparrow} - d_{z\uparrow} p_{z\downarrow} \right) + L^{pzpz}_0 |p_{z\downarrow} p_{z\uparrow}\rangle + \\ & L^{apz}_0 \left(a_\downarrow p_{z\uparrow} - a_\uparrow p_{z\downarrow} \right) + L^{dxdz}_0 \left(d_{x\downarrow} d_{z\uparrow} - d_{x\uparrow} d_{z\downarrow} \right) + \\ & L^{dxa}_0 \left(d_{x\downarrow} a_\uparrow - d_{x\uparrow} a_\downarrow \right) + L^{dxpz}_0 \left(d_{x\downarrow} p_{z\uparrow} - d_{x\uparrow} p_{z\downarrow} \right) + \\ & L^{dzb}_0 \left(d_{z\downarrow} b_\uparrow - d_{z\uparrow} b_\downarrow \right) + L^{ba}_0 \left(b_\downarrow a_\uparrow - b_\uparrow a_\downarrow \right) + \\ & L^{bpz}_0 \left(b_\downarrow p_{z\uparrow} - b_\uparrow p_{z\downarrow} \right) \end{aligned} \tag{8}$$

Table 2 Dependence of structural factors μ_{fg}, ν_{fg}, χ_{fg} [54, 73], λ_{fg}, ρ_{fg} from vector $\mathbf{R} = (R_x, R_y) = (f_x - g_x, f_y - g_y)$ connecting couple of sites f and g

R	μ_{fg}	ν_{fg}	λ_{fg}	ρ_{fg}	χ_{fg}
(0,0)	0.9580	0.72676	0.3729	0.4790	0
(1,0)	-0.1401	-0.2732	-0.0879	0.0588	-0.1339
(0,1)	-0.1401	-0.2732	-0.0879	-0.1989	0.1339
(1,1)	-0.0235	0.1221	0.0309	-0.0118	0
(2,0)	-0.0137	-0.0639	-0.0357	0.0127	0.0406
(0,2)	-0.0137	-0.0639	-0.0357	-0.0264	-0.0406
(2,1)	-0.0069	0.0174	0.0085	0.001	-0.0304
(1,2)	-0.0069	0.0174	0.0085	-0.0079	0.0304
(2,2)	-0.0033	0.0105	0.0046	-0.0016	0
(3,0)	-0.0035	-0.0169	-0.0175	0.0038	0.0277
(0,3)	-0.0035	-0.0169	-0.0175	-0.0073	-0.0277
(3,1)	-0.0026	0.0007	0.0027	0.0014	-0.0141
(1,3)	-0.0026	0.0007	0.0027	-0.0040	0.0141
(3,2)	-0.0016	0.0037	0.0022	-0.0000	-0.0031
(2,3)	-0.0016	0.0037	0.0022	-0.0016	0.0031
(3,3)	-0.0010	0.0024	0.0015	-0.0001	0

Hubbard Fermion Hoppings in the Orthorhombic Phase

Hamiltonian of the two-subband Hubbard model in the basis of quasiparticle excitations built on the four local cluster eigenstates (vacuum state $|0\rangle$, single hole states $|\sigma\rangle$ and $|\bar{\sigma}\rangle$, two-hole singlet state $|S\rangle$) has a form:

$$\begin{aligned} H = & \sum_f \varepsilon_0 X^{00}_f + \sum_{f\sigma} \left(\varepsilon_{1\sigma} - \mu \right) X^{\sigma\sigma}_f + \sum_f \left(\varepsilon_2 - 2\mu \right) X^{SS}_f + \\ & \sum_{fg\sigma} \sum_{pqmn} t_{fg\sigma}(pq, mn) X^{pq}_f X^{mn}_g \end{aligned} \tag{9}$$

where ε_0, ε_1, ε_2 are energies of cluster eigenstates with $n_h = 0, 1, 2$ holes respectively, μ is chemical potential. $t_{fg\sigma}(pq, mn) = \sum_{\lambda\lambda'} \sum_{pqmn} t_{\lambda\lambda'}(f, g) \gamma^*_{\lambda\sigma}(pq) \gamma_{\lambda'\sigma}(mn)$ is the inter-cluster quasiparticle hopping parameter. Hopping parameter $t_{fg\sigma}(pq, mn)$ characterizes process when cluster f goes from state q to state p acquiring hole which comes from cluster g transitioned from state n to state m. The matrix elements

$\gamma(pq)$ are the expansion coefficients of the electron annihilation operator in terms of Hubbard operators:

$$a_f = \sum_{pq} \langle p|a_f|q\rangle X_f^{pq} = \sum_{pq} \gamma(pq) X_f^{pq} \tag{10}$$

In the orthorhombic phase the expanded form of expression for $t_{fg\sigma}(pq, mn)$ looks like:

$$\begin{aligned}
&t_{fg\sigma}(pq, mn) = -2\left[t_{pd}\mu_{fg} + t_{pd}\rho_{fg}(\kappa - 1)\right]\times \\
&\left(\gamma^*_{dx\sigma}(pq)\gamma_{b\sigma}(mn) + \gamma^*_{b\sigma}(pq)\gamma_{dx\sigma}(mn)\right)+ \\
&2t_{pd}\lambda_{fg}(1-\kappa)\times \\
&\left(\gamma^*_{dx\sigma}(pq)\gamma_{a\sigma}(mn) + \gamma^*_{a\sigma}(pq)\gamma_{dx\sigma}(mn)\right)+ \\
&2\left[t_{pdz}\mu_{fg} - \left(1+\kappa'\right)\rho_{fg}t_{pdz}\right]\times \\
&\left(\gamma^*_{dz\sigma}(pq)\gamma_{b\sigma}(mn) + \gamma^*_{b\sigma}(pq)\gamma_{dz\sigma}(mn)\right)+ \\
&2\left(1+\kappa'\right)\lambda_{fg}t_{pdz}\times \\
&\left(\gamma^*_{dz\sigma}(pq)\gamma_{a\sigma}(mn) + \gamma^*_{a\sigma}(pq)\gamma_{dz\sigma}(mn)\right)+ \\
&2t_{pp}v_{fg}\left(-\gamma^*_{b\sigma}(pq)\gamma_{b\sigma}(mn) + \gamma^*_{a\sigma}(pq)\gamma_{a\sigma}(mn)\right)- \\
&2t_{pp}\chi_{fg}\left(\gamma^*_{b\sigma}(pq)\gamma_{a\sigma}(mn) + \gamma^*_{a\sigma}(pq)\gamma_{b\sigma}(mn)\right)+ \\
&2\left[t_{ppz}\mu_{fg} - (1+\beta)\rho_{fg}t_{ppz}\right]\times \\
&\left(\gamma^*_{b\sigma}(pq)\gamma_{pz\sigma}(mn) + \gamma^*_{pz\sigma}(pq)\gamma_{b\sigma}(mn)\right)- \\
&2t_{ppz}\lambda_{fg}(1+\beta)\times \\
&\left(\gamma^*_{a\sigma}(pq)\gamma_{pz\sigma}(mn) + \gamma^*_{pz\sigma}(pq)\gamma_{a\sigma}(mn)\right)
\end{aligned} \tag{11}$$

Presence of the terms with structural factors ρ_{fg} and χ_{fg} which have different values along the x- and y-axis in formula (11) results in dependence of $t_{fg\sigma}(pq, mn)$ on the direction of hopping. It is seen that $t_{fg\sigma}(pq, mn)$ in the orthorhombic phase contains plenty of terms. The reason for the appearance of these terms is that cluster eigenstates are a mix of orbitals of b_{1g} and a_{1g} symmetry in the orthorhombic phase and quasiparticle excitations $(0\bar{\sigma})$ and (σS) of Hubbard model with the origin of $d_{z\bar{\sigma}}, a_{\bar{\sigma}}, p_{z\bar{\sigma}}$ orbitals acquire nonzero probability.

Acknowledgements We would like to especially thank A. Bianconi for new ideas, useful discussions, and suggestions. We thank D.M. Dzebisashvili, I.A. Nekrasov, and A.A. Slobodchikov for valuable advice and useful discussions. The reported study was funded by Russian Foundation for Basic Research, Government of Krasnoyarsk Territory and Krasnoyarsk Regional Fund of Science according to the research project "Studies of superexchange and electron-phonon interactions in correlated systems as a basis for searching for promising functional materials" No. 20-42-240016.

References

1. Chu, C.W., Gao, L., Chen, F., Huang, Z.J., Meng, R.J., Xue, Y.Y.: Superconductivity above 150 K in $HgBa_2Ca_2Cu_3O_{8+\delta}$ at high pressures. Nature **365**, 323–325 (1993)
2. Gao, L., Xue, Y.Y., Chen, F., Xiong, Q., Meng, R.L., Ramirez, D., Chu, C.W., Eggert, J.H., Mao, H.K.: Superconductivity up to 164 K in $HgBa_2Ca_{m-1}Cu_mO_{2m+2+\delta}$ (m=1,2, and 3) under quasi-hydrostatic pressures. Phys. Rev. B **50**, 4260(R) (1994)
3. Hunter, B.A., Jorgensen, J.D., Wagner, J.L., Radaelli, P.G., Hinks, D.G., Shaked, H., Hitterman, R.L., Von Dreele, R.B.: Pressure-induced structural changes in superconducting $HgBa_2Ca_{n-1}Cu_nO_{2n+2+\delta}$ (n = 1, 2, 3) compounds. Physica C **221**, 1–10 (1994)
4. Aksenov, V.L., Balagurov, A.M., Savenko, B.N., Glazkov, V.P., Goncharenko, I.N., Somenkov, V.A., Antipov, E.V., Putilin, S.N., Capponi, J.J.: Neutron diffraction study of the high-temperature superconductor $HgBa_2CaCu_2O_{6.3}$ under high pressure. High Press. Res. **14**, 127-137 (1995)
5. Armstrong, A.R., David, W.I.F., Gameson, I., Edwards, P.P., Capponi, J.J., Bordet, P., Marezio, M.: Crystal structure of $HgBa_2Ca_2Cu_3O_{8+\delta}$ at high pressure (to 8.5 GPa) determined by powder neutron diffraction. Phys. Rev. B **52**, 15551-15557 (1995)
6. Cao, Y., Xiong, Q., Xue, Y.Y., Chu, C.W.: Pressure effect on the T_c of $HgBa_2CuO_{4+\delta}$ with $0.07 \leq \delta \leq 0.39$. Phys. Rev. B **52**, 6854-6857 (1995)
7. Aksenov, V.L., Balagurov, A.M., Savenko, B.N., Sheptyakov, D.V., Glazkov, V.P., Somenkov, V.A., Shilshtein, SSh., Antipov, E.V., Putilin, S.N.: Investigation of the $HgBa_2CuO_{4+\delta}$ structure under external pressures up to 5 GPa by neutron powder diffraction. Physica C **275**, 87–92 (1997)
8. Qiu, X.D., Xiong, Q., Gao, L., Cao, Y., Xue, Y.Y., Chu, C.W.: Pressure dependence of T_c in $HgBa_2CuO_{4+\delta}$ up to 18 GPa with $0.17 < \delta < 0.3$. Physica C **282-287**, 885-886 (1997)
9. Núñez-Regueiro, M., Acha, C.: Resistivity measurements on high temperature superconductors at high pressures. In: Narlikar, A.V. (ed.) Studies of High Temperature Superconductors, pp. 203–232. Nova Science Publishers, New York (1997)
10. Acha, C., Núñez-Regueiro, M., Le Floch, S., Bordet, P., Capponi, J.J., Chaillout, C., Tholence, J.L.: Overdoped $Hg_{1-x}Au_xBa_2Ca_2Cu_3O_{8+x}$, the origin of the intrinsic increase of T_c under pressure in mercury cuprates. Phys. Rev. B **57**, R5630–R5633 (1998)
11. Balagurov, A.M., Sheptyakov, D.V., Aksenov, V.L., Antipov, E.V., Putilin, S.N., Radaelli, P.G., Marezio, M.: Structure of $HgBa_2CuO_{4+\delta}$ ($0.06< \delta <0.19$) at ambient, high pressure. Phys. Rev. B **59**, 7209-7215 (1999)
12. Lokshin, K.A., Pavlov, D.A., Putilin, S.N., Antipov, E.V., Sheptyakov, D.V., Balagurov, A.M.: Enhancement of T_c in $HgBa_2Ca_2Cu_3O_{8+\delta}$ by fluorination. Phys. Rev. B **63**, 064511 (2001)
13. Antipov, E.V., Abakumov, A.M., Putilin, S.N.: Chemistry, structure of Hg-based superconducting Cu mixed oxides. Supercond. Sci. Tech. **15**, R31–R49 (2002)
14. Plakida, N.P.: High-Temperature Cuprate Superconductors. Springer-Verlag, Berlin, Heidelberg (2010)
15. Kraut, O., Meingast, C., Bräuchle, G., Claus, H., Erb, A., Müller-Vogt, G., Wühl, H.: Uniaxial pressure dependence of T_c of untwinned $YBa_2Cu_3O_x$ single crystals for x=6.5-7. Physica C **205**, 139-146 (1993)
16. Meingast, C., Kraut, O., Wolf, T., Wühl, H., Erb, A., Müller-Vogt, G.: Large *a-b* anisotropy of the expansivity anomaly at T_c in untwinned $YBa_2Cu_3O_{7-\delta}$. Phys. Rev. Lett. **67**, 1634–1637 (1991)
17. Hardy, F., Hillier, N.J., Meingast, C., Colson, D., Li, Y., Barišić, N., Yu, G., Zhao, X., Greven, M., Schilling, J.S.: Enhancement of the Critical Temperature of $HgBa_2CuO_{4+\delta}$ by Applying Uniaxial, Hydrostatic Pressure: Implications for a Universal Trend in Cuprate Superconductors. Phys. Rev. Lett. **105**, 167002 (2010)
18. Gugenberger, F., Meingast, C., Roth, G., Grube, K., Breit, V., Weber, T., Wühl, H., Uchida, S., Nakamura, Y.: Uniaxial pressure dependence of T_c from high-resolution dilatometry of untwinned $La_{2-x}Sr_xCuO_4$ single crystals. Phys. Rev. B **49**, 13137–13142 (1994)
19. Meingast, C., Junod, A., Walker, E.: Superconducting fluctuations, uniaxial-pressure dependence of T_c of a $Bi_2Sr_2CaCu_2O_{8+x}$ single

crystal from high-resolution thermal expansion. Physica C **272**, 106–114 (1996)
20. Schilling, J.S., Klotz, S.: The Influence of High Pressure on the Superconducting and Normal State Properties of High Temperature Superconductors. In: Ginsberg, D.M. (ed.) Physical Properties of High Temperature Superconductors III, pp. 59–157. World Scientific, Singapore (1992)
21. Loquet, J.P., Perret, J., Fompeyrine, J., Mächler, E., Seo, J.W., Van Tendeloo, G.: Doubling the critical temperature of $La_{1.9}Sr_{0.1}CuO_4$ using epitaxial strain. Nature **394**, 453-456 (1998)
22. Sun, G.F., Wong, K.W., Xu, B.R., Xin, Y., Lu, D.F.: T_c enhancement of $HgBa_2Ca_2Cu_3O_{8+\delta}$ by Tl substitution. Phys. Lett. A **192**, 122–124 (1994)
23. Dai, P., Chakoumakos, B.C., Sun, G.F., Wong, K.W., Xin, Y., Lu, D.F.: Synthesis, neutron powder diffraction study of the superconductor $HgBa_2Ca_2Cu_3O_{8+\delta}$ by Tl substitution. Physica C **243**, 201–206 (1995)
24. Bryntse, I.: A review of the synthesis and properties of Hg-containing superconductors, focused on bulk materials and thin films. In: Narlikar, A. (ed.) High Temperature Superconductors, pp. 1–27. Nova Science Book Series, New York (1997)
25. Attfield, J.P., Kharlanov, A.L., McAllister, J.A.: Cation effects in doped La_2CuO_4 superconductors. Nature (London) **394**, 157–159 (1998)
26. Eisaki, H., Kaneko, N., Feng, D.L., Damascelli, A., Mang, P.K., Shen, K.M., Shen, Z.X., Greven, M.: Effect of chemical inhomogeneity in bismuth-based copper oxide superconductors. Phys. Rev. B **69**, 064512 (2004)
27. Fujita, K., Noda, T., Kojima, K.M., Eisaki, H., Uchida, S.: Effect of Disorder Outside the CuO_2 Planes on T_c of Copper Oxide Superconductors. Phys. Rev. Lett. **95**, 097006 (2005)
28. Gao, W.B., Liu, Q.Q., Yang, L.X., Yu, Y., Li, F.Y., Jin, C.Q., Uchida, S.: Out-of-plane effect on the superconductivity of $Sr_{2-x}Ba_xCuO_{3+\delta}$ with T_c up to 98 K. Phys. Rev. B **80**, 094523 (2009)
29. Welp, U., Grimsditch, M., Fleshler, S., Nessler, W., Downey, J., Crabtree, G.W., Guimpel, J.: Effect of uniaxial stress on the superconducting transition in $YBa_2Cu_3O_7$. Phys. Rev. Lett. **69**, 2130–2133 (1992)
30. Watanabe, N., Fukamachi, K., Ueda, Y., Tsushima, K., Balashov, A.M., Nakanishi, T., Mori, N.: Effect of hydrostatic and uniaxial stress on T_c for single crystals of $Bi_2Sr_2CaCu_2O_x$. Physica C **235–240**, 1309–1310 (1994)
31. Fernandes, A.A.R., Santamaria, J., Bud'ko, S.L., Nakamura, O., Guimpel, J., Schuller, I.K.: Effect of physical, chemical pressure on the superconductivity of high-temperature oxide superconductors. Phys. Rev. B **44**, 7601–7606 (1991)
32. Takahashi, H., Shaked, H., Hunter, B.A., Radaelli, P.G., Hitterman, R.L., Hinks, D.G., Jorgensen, J.D.: Structural effects of hydrostatic pressure in orthorhombic $La_{2-x}Sr_xCuO_4$. Phys. Rev. B **50**, 3221–3229 (1994)
33. Goko, T., Nakamura, F., Fujita, T.: Reduction of Superconducting Transition Temperature due to Orthorhombic Distortion in $La_{2-x}Sr_xCuO_4$. J. Phys. Soc. Jpn. **68**, 3074–3077 (1999)
34. Agrestini, S., Saini, N.L., Bianconi, G., Bianconi, A.: The strain of CuO_2 lattice: the second variable for the phase diagram of cuprate perovskites. J. Phys. A: Math. Gen. **36**, 9133–9142 (2003)
35. Plakida, N.M.: Antiferromagnetic exchange mechanism of superconductivity in cuprates. JETP Lett. 74, 36–40 (2001)
36. Sidorov, K.A., Gavrichkov, V.A., Nikolaev, S.V., Pchelkina, Z.V., Ovchinnikov, S.G.: Effect of external pressure on the normal and superconducting properties of high-T_c cuprates. Phys. Status Solidi B **253**, 486–493 (2016)
37. Makarov, I.A., Gavrichkov, V.A., Shneyder, E.I., Nekrasov, I.A., Slobodchikov, A.A., Ovchinnikov, S.G., Bianconi, A.: Effect of CuO_2 Lattice Strain on the Electronic Structure and Properties of High-T_c Cuprate Family. J. Supercond. Novel Magn. **32**, 1927–1935 (2019)
38. King, D.M., Shen, Z.X., Dessau, D.S., Marshall, D.S., Park, C.H., Spicer, W.E., Peng, J.L., Li, Z.Y.,Greene, R.L.: Observation of a Saddle-Point Singularity in $Bi_2(Sr_{0.97}Pr_{0.03})_2CuO_{6+\delta}$ and Its Implications for Normal and Superconducting State Properties. Phys. Rev. Lett. **73**, 3298-3301 (1994)
39. Ino, A., Kim, C., Mizokawa, T., Shen, Z.X., Fujimori, A., Takaba, M., Tamasaku, K., Eisaki, H., Uchida, S.: Fermi Surface and Band Dispersion in $La_{2-x}Sr_xCuO_4$. J. Phys. Soc. Jpn. **68**, 1496–1499 (1999)
40. Shneyder, E.I., Ovchinnikov, S.G., Korshunov, M.M., Nikolaev, S.V.: Electronic structure and properties of high-T_c superconducting cuprates in the normal and superconducting phases within the LDA + GTB approach. JETP Lett. **96**, 349–360 (2012)
41. Timusk, T., Statt, B.: The pseudogap in high-temperature superconductors: an experimental survey. Rep. Prog. Phys. **62**, 61–122 (1999)
42. Damascelli, A., Hussain, Z., Shen, Z.X.: Angle-resolved photoemission studies of the cuprate superconductors. Rev. Mod. Phys. **75**, 473–541 (2003)
43. Zhou, X.J., Cuk, T., Devereaux, T., Nagaosa, N., Shen, Z.X.: Angle-Resolved Photoemission Spectroscopy on Electronic Structure and Electron-Phonon Coupling in Cuprate Superconductors. In: Schrieffer, J.R., Brooks, J.S. (eds.) Handbook of High-Temperature Superconductivity, pp. 87–144. Springer, New York (2007)
44. Vishik, M., Lee, W.S., He, R.H., Hashimoto, M., Hussain, Z., Devereaux, T.P., Shen, Z.X.: ARPES studies of cuprate Fermiology: superconductivity, pseudogap and quasiparticle dynamics. New J. Phys. **12**, 105008 (2010)
45. Kordyuk, A.A.: Pseudogap from ARPES experiment: Three gaps in cuprates and topological superconductivity. Low Temp. Phys. **41**, 319–341 (2015)
46. Keimer, B., Kivelson, S.A., Norman, M.R., Uchida, S., Zaanen, J.: From quantum matter to high-temperature superconductivity in copper oxides. Nature **518**, 179–186 (2015)
47. Vishik, I.M.: Photoemission perspective on pseudogap, superconducting fluctuations and charge order in cuprates: a review of recent progress. Rep. Progr. Phys. **81**, 062501 (2018)
48. Sénéchal, D., Perez, D., Pioro-Ladrière, M.: Spectral Weight of the Hubbard Model through Cluster Perturbation Theory. Phys. Rev. Lett. **84**, 522–525 (2000)
49. Sénéchal, D., Tremblay, A.-M.S.: Hot Spots, Pseudogaps for Hole- and Electron-Doped High-Temperature Superconductors. Phys. Rev. Lett. **92**, 126401 (2004)
50. Ovchinnikov, S.G., Shneyder, E.I.: Spectral functions in the Hubbard model with half-filling. Phys. Solid State **46**, 1469–1473 (2004)
51. Kuchinskii, E.Z., Nekrasov, I.A., Sadovskii, M.V.: Pseudogaps: introducing the length scale into dynamical mean-field theory. Low Temp. Phys. **32**, 398–405 (2006)
52. Plakida, N.M., Oudovenko, V.S.: Electron spectrum in high-temperature cuprate superconductors. J. Exp. Theor. Phys. **104**, 230–244 (2007)
53. Ovchinnikov, S.G., Sandalov, I.S.: The band structure of strong-correlated electrons in $La_{2-x}Sr_xCuO_4$, $YBa_2Cu_3O_{7-y}$. Physica C **161**, 607–617 (1989)
54. Gavrichkov, V.A., Ovchinnikov, S.G., Borisov, A.A., Goryachev, E.G.: Evolution of the band structure of quasiparticles with doping in copper oxides on the basis of a generalized tight-binding method. J. Exp. Theor. Phys. **91**, 369–383 (2000)
55. Korshunov, M.M., Gavrichkov, V.A., Ovchinnikov, S.G., Pchelkina, Z.V., Nekrasov, I.A., Korotin, M.A., Anisimov, V.I.: Parameters of the effective singlet-triplet model for band structure of high-T_c cuprates by alternative approaches. J. Exp. Theor. Phys. **99**, 559–565 (2004)

56. Korshunov, M.M., Gavrichkov, V.A., Ovchinnikov, S.G., Nekrasov, I.A., Pchelkina, Z.V., Anisimov, V.I.: Hybrid LDA, generalized tight-binding method for electronic structure calculations of strongly correlated electron systems. Phys. Rev. B. **72**, 165104 (2005)
57. Ovchinnikov, S.G.: Quasiparticles in strongly correlated electron systems in copper oxides. Usp. Fiz. Nauk **40**, 993–1017 (1997)
58. Plakida, N.M., Anton, L., Adam, S., Adam, G.: Exchange, spin-fluctuation mechanisms of superconductivity in cuprates. J. Exp. Theor. Phys. **97**, 331–342 (2003)
59. Sigrist, M., Rice, T.M.: Symmetry classification of states in high temperature superconductors. Z. Phys. B.: Condensed Matter **68**, 9-14 (1987)
60. Sigrist, M., Ueda, K.: Phenomenological Theory of unconventional superconductivity. Rev. Mod. Phys. **63**, 239–311 (1991)
61. Mineev, V.P., Samohin, K.V.: Introduction to theory of unconventional superconductivity. MPhTI, Moscow (1998)
62. Kirtley, J.R., Tsuei, C.C., Ariando, A., Verwijs, C.J.M., Harkema, S., Hilgenkamp, H.: Angle-resolved phase-sensitive determination of the in-plane gap symmetry in $YBa_2Cu_3O_{7-\delta}$. Nature Phys. **2**, 190–194 (2006)
63. Smilde, H.J.H., Golubov, A.A., Ariando, Rijnders, G., Dekkers, J.M., Harkema, S., Blank, D.H.A., Rogalla, H., Hilgenkamp, H.: Admixtures to d-Wave Gap Symmetry in Untwinned $YBa_2Cu_3O_7$ Superconducting Films Measured by Angle-Resolved Electron Tunneling. Phys. Rev. Lett. **95**, 257001 (2005)
64. Val'kov, V.V., Dzebisashvili, D.M.: Modification of the superconducting order parameter $\Delta(k)$ by long-range interactions. JETP Lett. **77**, 381–384 (2003)
65. Val'kov, V.V., Dzebisashvili, D.M., Korovushkin, M.M., Barabanov, A.F.: Coulomb repulsion of holes and competition between $d_{x^2-y^2}$-wave and *s*-wave parings in cuprate superconductors. J. Exp. Theor. Phys. **125**, 810–821 (2017)
66. Bianconi, A.: On the possibility of new high T_c superconductors by producing metal heterostructures as in the cuprate perovskites. Sol. State Commun. **89**, 933–936 (1994)
67. Bianconi, A., Missori, M., Saini, N.L., Oyanagi, H., Yamaguchi, H., Ha, D.H., Nishihara, Y.: High critical temperature in a superlattice of quantum wires. J. Supercond. **8**, 545–548 (1995)
68. Bianconi, A., Missori, M., Oyanagi, H., Yamaguchi, H., Ha, D.H., Nishihara, Y., Della Long, S.: The Measurement of the Polaron Size in the Metallic Phase of Cuprate Superconductors. Europhys Lett. **31**, 411–415 (1995)
69. Bianconi, A., Saini, N.L., Lanzara, A., Missori, M., Rossetti, T., Oyanagi, H., Yamaguchi, H., Oka, K., Ito, T.: Determination of the Local Lattice Distortions in the CuO_2 Plane of $La_{1.85}Sr_{0.15}CuO_4$. Phys. Rev. Lett. **76**, 3412-3415 (1996)
70. Saini, N.L., Lanzara, A., Oyanagi, H., Yamaguchi, H., Oka, K., Ito, T., Bianconi, A.: Local lattice instability and stripes in the CuO_2 plane of the $La_{1.85}Sr_{0.15}CuO_4$ system by polarized XANES and EXAFS. Phys. Rev. B **55**, 12759-12769 (1997)
71. Wakimoto, S., Shirane, G., Endoh, Y., Hirota, K., Ueki, S., Yamada, K., Birgeneau, R.J., Kastner, M.A., Lee, Y.S., Gehring, P.M., Lee, S.H.: Observation of incommensurate magnetic correlations at the lower critical concentration for superconductivity in $La_{2-x}Sr_xCuO_4$ (x=0.05). Phys. Rev. B **60**, R769-R772 (1999)
72. Shastry, B.S.: t-J model and nuclear magnetic relaxation in high-T_c materials. Phys. Rev. Lett. **63**, 1288–1291 (1989)
73. Raimondi, R., Jefferson, J.H., Feiner, L.F.: Effective single-band models for the high-T_c cuprates. II. Role of apical oxygen. Phys. Rev. B **53**, 8774-8788 (1996)